공학석사학위논문

Rapid aggregation of cells via vertical vibration

연직 진동을 이용한 세포의 고속 응집

2023 년 8 월

서울대학교 대학원

기계공학부

황 재 우

Rapid aggregation of cells via vertical vibration

연직 진동을 이용한 세포의 고속 응집

지도교수 김 호 영

이 논문을 공학석사 학위논문으로 제출함

2023 년 4 월

서울대학교 대학원

기계공학부

황 재 우

황재우의 공학석사 학위논문을 인준함

2023 년 6 월

위 원 장 : _____ **(인)**

부위원장 : _____ **(인)**

위 원 : _____ **(인)**

Abstract

최근 암을 정복하기 위한 신약개발이 활발히 진행되고 있다. 신약 개발 과정에서 임상 시험 진행 전까지는, 암세포들이 응집하여 신체조직과 비슷한 기능을 하는 세포 응집체(spheroid)에 약의 효용성을 확인한다.

세포 응집체는 세포가 자랄 수 있는 배양액 환경 속에서, 세포들을 한 점으로 모은 뒤 세포 사이의 결합을 유도하는 방식으로 제작한다. 세포를 한 점으로 모으는 과정에서 많은 시간이 걸려, 신약 개발 과정에서 많은 비용을 초래하여 왔다. 최근까지 다양한 방식(초음파 이용, 중력 이용, 배치(batch) 형식의 반응기 이용, 전자기장 이용 등)을 이용해서 세포 응집체를 제작하였으나, 제작 시간이 충분히 단축되지 않거나 세포들의 생존 능력(viability)을 저해하곤 해서, 현재까지도 세포 응집체의 제작 과정은 신약 개발의 주요 장애물로 여겨진다.

본 연구에서는, 유체에 연직 방향의 진동(vertical vibration)을 가할 때 생기는 유동을 이용하여 세포의 빠르게 응집하는 현상을 탐구하였다. 기존에 평면 구조에서만 관찰되던, 연직 진동 하의 streaming flow를 축대칭(axis-symmetry) 형상에서도 발견하였고, 이 유동장이 세포를 빠르고 조밀하게 모으는 것을 확인하였다. 이후, 이론 및 시뮬레이션 분석을 통해, 해당 유동이 어떻게 발생하고 어떻게 세포를 모으는 데 효과적인지 분석하였다. 또한, 해당 유동을 이용하여 실제로 세포를 응집시켜 세포 응집체를 만들고, 세포의 생존 능력에 큰 문제가 없음을 확인하였다. 다른 방법과의 비교를 통해, 본 연구의 방법이 더 빠르고 조밀하게 세포를 모으는 것도 확인하였다.

주요어 : 세포 응집체, 연직 진동, 패러데이 수면파, streaming flow, cell aggregation, spheroid

학 번 : 2021-27838

Table of Contents

List of Figures

Introduction

1. Research Backgrounds

Recently, due to the dramatic increase on the human's self-awareness of one's health, coupled with the drastic development of medical technologies, humans are living longer expected life than ever. However, as the average age increases rapidly, the possibility of genetic mutations escalates steeply; some genetic mutations, which cannot regulate its growth, develops as cancer. The occurrence rate of cancer shows drastic increase in the few years; the problem could get more serious since the expected age increases continuously and those societies are normally aging. Therefore, the drugs treating cancers are being developed competitively in many firms, labs and universities globally; the market size was estimated near 138.41 billion US dollars in 2022.

When developing the cancer drugs, the efficacy of the drug should be confirmed before being subjected to a clinical trial. Most of the testing of the drugs are conducted by spheroids: cancer cell aggregates that function similarly

to body tissues.

Spheroids are produced by inducing cell aggregation in a culture medium environment where cells can grow. It takes a long time to gather the cells together into one point, which has caused high inefficacy during cancer drug development. Although various methods (using ultrasound, gravity, batch-type reactors, electric fields and magnetic fields, etc.) have been used to produce spheroids, the production time has not been shortened enough or has impaired the viability of cells so far. Therefore, the rapid but cell-habitable production of spheroids is still regarded as a major obstacle in cancer drug development.

In this study, we investigated the phenomenon of rapid cell aggregation using flow field generated by the interaction of vertical vibration and surface tension. We found that a streaming flow arises due to the moderate Reynolds number of the vibration system, and the streaming flow showed perfect axisymmetry under vertical vibration. Conducting experiments with real cancer cells, we found out that this axisymmetric, point-directing flow can rapidly and densely gather the cells in the desired point. In addition, we created spheroids and confirmed that there were no major problems with cell viability as well. Through comparison with other methods, it was also proved that this method

gathers cells faster and more densely. Subsequently, we analyzed how this flow is generated and how it makes the cells gather, through theoretical explanation and CFD simulations.

2. Research Objective

The main object of this research is to develop a new process for rapid production of cell spheroids, while not diminishing its viability. The secondary object of the research is to analyze the discovered flow field and identify the cause of the cell aggregation. Due to the complex nature of the flow field and its interaction with the cells (transient system, the importance of non-linear terms, contact angle hysteresis and contact line motion, rotation and distortion of individual cells, etc.), the analysis will mainly be introduced in a qualitative form.

Subject

1. Streaming flow induced by vertical vibration

When a sinusoidal vibration is exerted to linear systems, the system variables will show a time averaged value of zero. However, for non−linear systems, the non−linear response induced by the input oscillation accumulates in the system, generating a non−zero time average of some variables. For liquid systems, the Navier−Stokes equation governs the system.

$$\rho \frac{\partial u_i}{\partial t} + \rho u_i \cdot \nabla u_i = -\nabla p + \mu \nabla^2 u_i + \rho b_i$$

For liquid systems with non−negligible inertial effects (i.e. when the Reynolds number, $Re \gtrsim 1$), the governing equation for the liquid system remains nonlinear due to the inertial term. Therefore, when oscillation is exerted on the system, the time averaged velocity will show a non−zero average. The averaged flow (mean flow) is termed as streaming flow. The phenomenon can be

observed in various systems such as simple vertical, horizontal vibration of fluids, fluid acoustics, and alligator communications.

Faraday wave, which is named after the physicist Michael Faraday, is a standing wave which emerges under vibration of liquids with free surface. When the acceleration (or frequency) of vibration exceeds its innate threshold value, some instability occurs on the free surface and it tends to distort itself, generating standing waves. Under the Faraday waves, streaming flow occurs when the Faraday waves are large enough to consider the inertial terms in the Navier–Stokes equation notable.

The wavelength of the standing waves is determined by its frequency, water depth, surface tension and liquid density. Under normal Faraday wave setup, the variables are constant along the liquid system: the wavelength is same for all standing waves, indicating that the waves are evenly spaced. Under the periodic standing waves, the streaming flow also showed periodic behavior in the form of periodic vortices. For a detailed research on the streaming flow under the waves, please refer to ~~.

Replicating the Faraday wave streaming flow experiments that ~ conducted,

the observations showed that the seeding particles for the flow field analysis aggregated at the bottom between the vortices. Two types of aggregates were formed according to their position relative to the vortices: for the vortices under the upward streaming flow, very sharp, dense aggregate of particles were formed; in contrary, for the vortices under the downward streaming flow, rather coarse aggregate was formed. The research aims to exploit this phenomenon in cell aggregation.

Figure 1. Particle aggregation under Faraday waves in rectangular tanks. Two types of particle gathering, coarse (green) and compact (red) occurs.

2. Axisymmetric streaming flow in cylindrical wells

2.1. 96 well plate format

Most of the cancer drug testing researches share the same experiment format of 96 microwell plates. The devices such as automated pipets, microscopes, and incubating systems are fitted for the 96 well standards. Therefore, for accessibility in the drug development industry, the system should be compatible to the conventional 96 well system.

96 well plates have cylindrical geometry, so the Faraday wave and the streaming flow pattern exert distinct behaviors. Experiments were conducted to observe how the standing waves and the streaming flow underneath the flow emerges.

2.2 Experimental setup

The vibration experiment was conducted for liquids inside cylindrical wells of 96 well formats. The experimental setup was set as **Figure 2**. The shaker was placed on top of an optical table to minimize the background vibration. The shaker used for the experiment was Electrodynamic Shaker ET-140 (Labworks Inc.). The shaker was connected to an electric signal generator and an amplifier. Also, the shaker was always cooled with a vacuum pump. Laser sheet from the top penetrated the cross section of the liquid in the well. High-speed camera (Fastcam SA1.1, Photron Inc.) was mounted in the normal direction to the cross section of the laser sheet. To adjust the laser sheet thickness, a controllable laser sheet adjusting device was attached under the laser. The wells were mounted mechanically on top of the vibrator. The whole apparatus was shaded to minimize the distraction from other light sources.

The cell culture medium was mixed with 1% Matrigel (Corning Inc.), and the cells were mixed in the concentration of 0.067 million cells/mL. The viscosity measured was 1.51 mPas, and the surface tension measured was 42 mN/m. The density was 0.96 kg/m3. All measurements were conducted in room

temperature of 25 deg C. The cells used was HT−29, which is a colon cancer cell. Two types of HT−29 cells were used: normal HR−29 cells and green−fluorescent protein tagged cells. Negligible amount of fluorescent polystyrene particles, diameter of 10 um and density of 1.08 kg/m3, provided by Magsphere Inc., was added to the solution when analyzing the flow field.

The vibration condition was the frequency of 50 Hz with the amplitude of 0.2 mm.

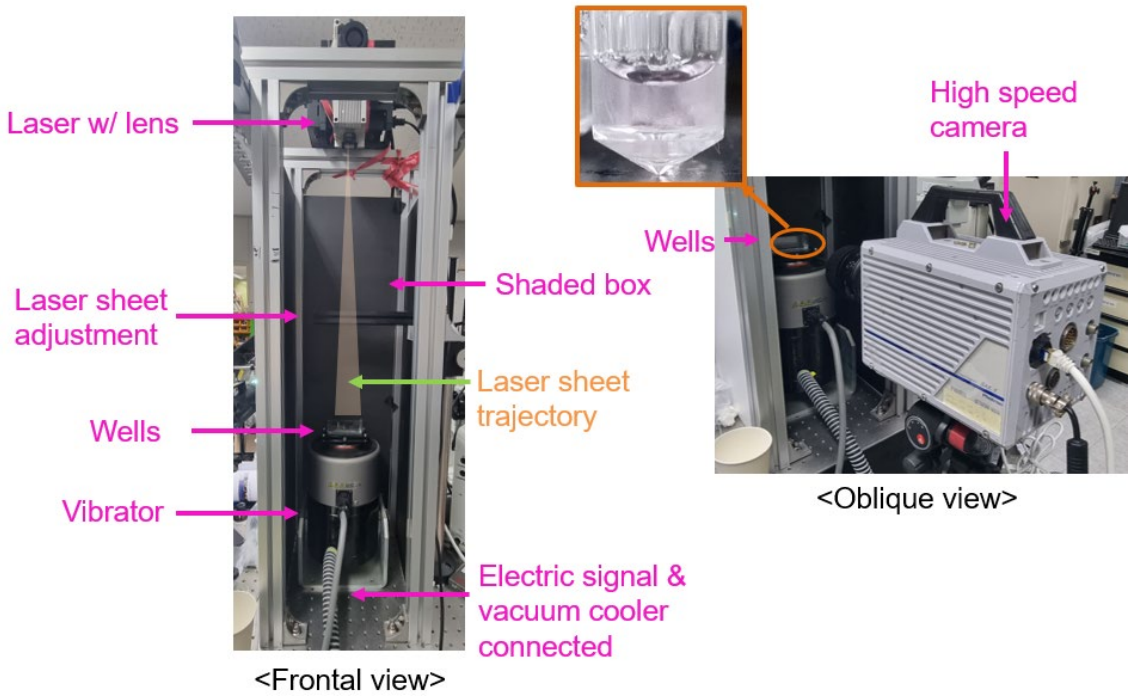

Figure 2. The experimental setup. Shown left is the frontal view and the right is the oblique view, showing the wells and high-speed camera.

2.3. Contact line observation

Subjected to vertical vibration, the liquid inside the well shows some peculiar motion inside the well. To alleviate the optical illusion caused by the vibration of the wells, a simple modification on the image was performed to fix the bottom of the well in the same position of the image.

The evolution of surface, its height and contact angle hysteresis, is the first thing to note.

During vibration, the surface tends distort, oscillating between the nearly-flat state and the curved state. (**Figure 3. 4**) To satisfy volume conservation, if the center of the surface goes up (or down), the contact line goes down (or up). Here we set the height of the meniscus center as the representative variable of the meniscus height. Upon observation, it can be checked that the height of the meniscus center has a phase lead of $\frac{\pi}{2}$ compared to the height of the well. When the well height was in its equilibrium, the velocity of the contact line center was at its maximal value.

The contact angle shows different behavior depending on its velocity. When the center of the meniscus is going down, the contact line inclines upwards,

where the liquid is not present. Therefore, the contact angle is in its advancing state which is larger than the equilibrium contact angle. When the center of the meniscus is going up, the contact line declines downward. Here, the contact line is in its receding state and the contact angle gets smaller than its equilibrium value.

To wrap up the complicated phase relationship, the relationship can be summarized as below:

① By observation, the meniscus center height shows $\frac{\pi}{2}$ phase lead compared to the well height

② The contact line height as opposite phase compared to meniscus center height, meaning that it has $\frac{\pi}{2}$ phase lag compared to the well height

③ The contact line velocity has $\frac{\pi}{2}$ phase lead compared to the well height, meaning that it is in the same phase with the well height

④ When the contact line velocity is positive, the contact line advances, and the contact angle increase, vice versa. Therefore, the contact angle is in the same phase with contact line velocity

⑤ Contact angle is in the same phase with the well height

For more intuitive and apparent explanation, the system can be explained by exploiting sinusoidal functions.

Starting by assuming the meniscus center height as a sine function,

$$y_{meniscus\ center} \sim \sin t$$

From observation, the well height has a phase lag of $\frac{\pi}{2}$; therefore, the well height can be represented as below.

$$y_{well\ height} \sim -\cos t$$

To satisfy volume conservation of liquids, the contact line height will show opposite phase compared to the meniscus center.

$$y_{contact\ line} \sim -\sin t$$

The contact line velocity is obtained by the first derivative of the contact line height.

$$\frac{dy_{contact\ line}}{dt} \sim -\cos t$$

Contact line velocity and contact angle has positive relationship (**Figure 4**): therefore, the contact angle is in the same phase with the contact line velocity.

$$\theta_{contact\ angle} \sim -\cos t$$

Therefore, it is can be concluded that the contact angle is in the same phase with the well height. More complicated analysis of these relationships will be

dealt on the analysis and the simulation in section 4.

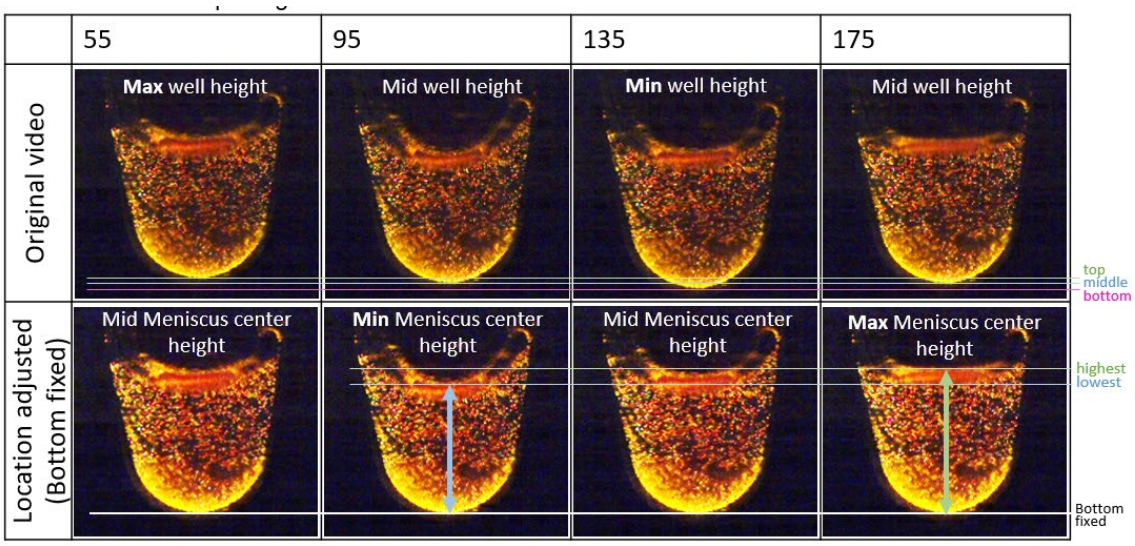

Figure 3. Location adjustment of the well

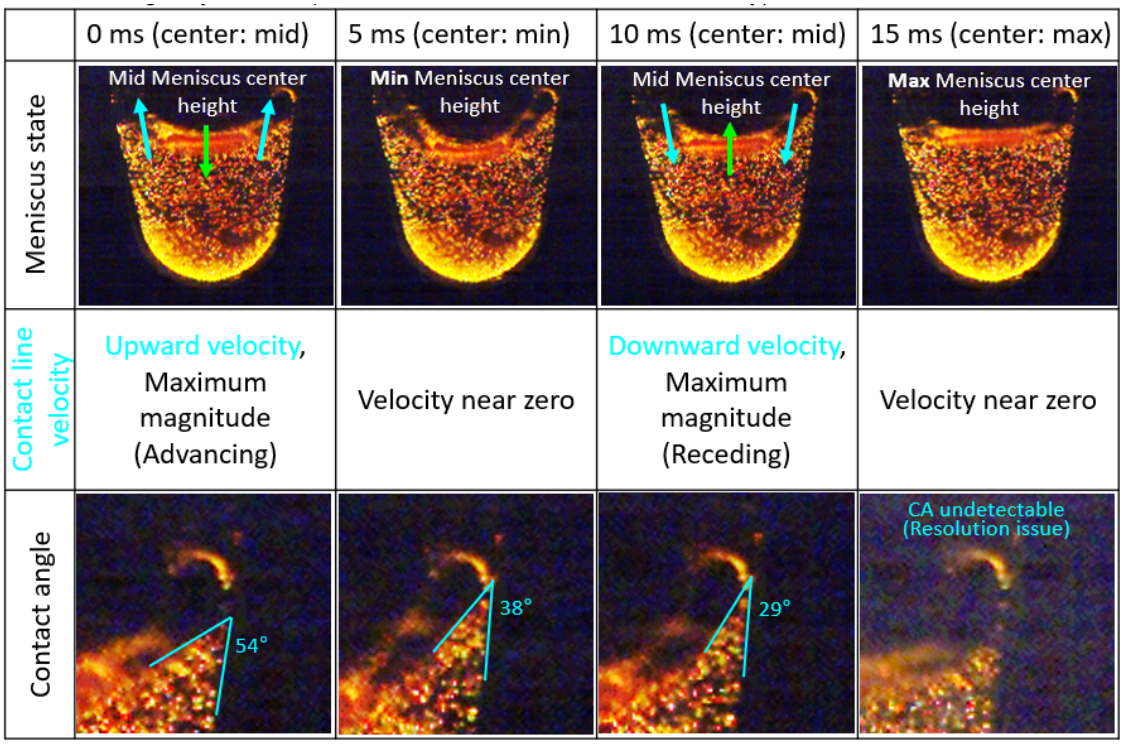

Figure 4. The evolution of surface and its corresponding contact angle hysteresis. The diameter of the well is 8 mm

2.4. Flow field observation

The flow field was observed by discharging laser at the fluorescent liquid particles. Similar to the contact line observation, the vibration was adjusted by image analysis. To check whether the particles correctly represents the fluid flow, the Stokes number should be checked in advance. The characteristic velocity of the system is $u_{char} = \frac{2A}{T/2}$. Inserting the amplitude (0.2 mm) and the period (0.02 second), the characteristic speed can be obtained as $u_{char} = 0.04\ m/s$. Inserting the value in the Stokes number relationship for low Reynolds flow, the Stokes number can be obtained. The computed value is $St = \frac{\rho D u_{char}}{18\mu} = 0.02 \ll 1$: therefore, it could be assured that the particle readily follows the streamline.

First, focus on the vibration in one period. During one period, the flow tends to follow the surface movement. Fluid elements those are near to the surface moves vigorously, while the fluid elements near the bottom wall moves very slowly, due to the no-slip condition. During one period, the particles seems to go back to its initial state: in the pixel limit of high-speed camera, it is nearly insignificant. Also, the pixel limit is insufficient for tracking the slowly moving

particle near the bottom, in which the flow is most important for cell aggregation.

Secondly, focus on the average flow. For this analysis, instead of obtaining the time averaged velocity throughout the whole period, the same phase points in every period were collected and combined into a video. Under the assumption that the time averaged flow (streaming flow) is steady throughout the whole time, the combined video can be an effective way to visualize the video. The mean flow field indicates that, the mean flow field is symmetric. At the middle, a downward-directing mean flow develops, and near the upper part of the center, two symmetric vortices (actually, they are one torus-shaped vortex) are present. Near the contact line, symmetric secondary vortices rotate in the opposite direction.

Even though the fluorescent particles have similar density and size with the HT-29 cells, the degree of wall attachment varies largely between the fluorescent particles and the cells: the anti-sticking well plates refrain the cells from sticking, but the particles stick easily. Therefore, the in-situ tracking of the particle density was not possible.

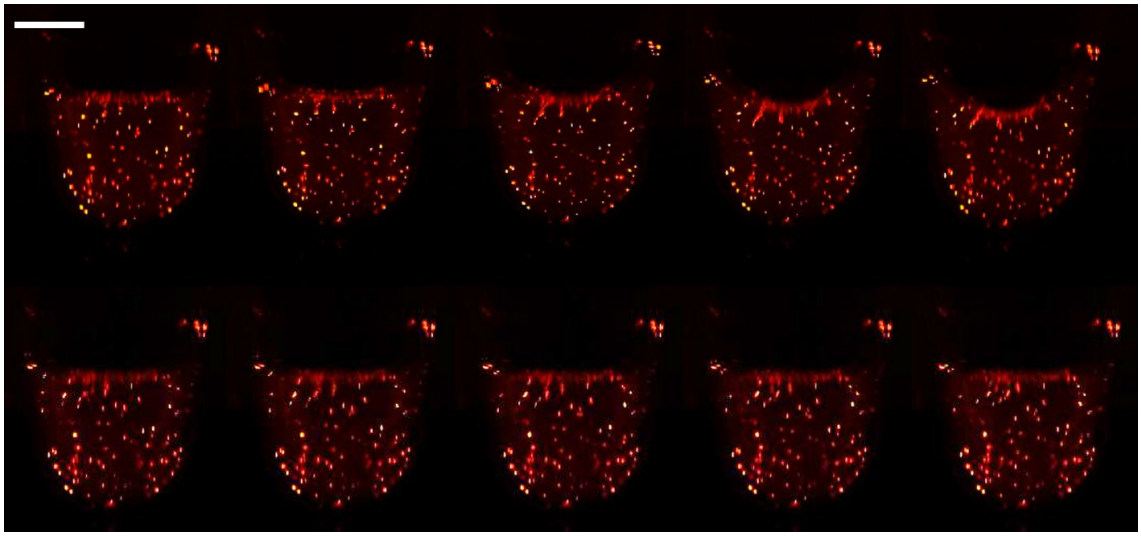

Figure 5. (Top) The evolution of meniscus within half period (10 ms). (Bottom) The average flow (5 periods) Scale bar 3 mm

3. Cell aggregation under vertical vibration

3.1. Temporal evolution of cell aggregates

In this section, the results of experiments containing cells are presented. The well tested is a commercial ultra-low adhesive well (PrimeSurface 96M plate, Sbio Inc., Japan) which refrain cells from sticking to the wells.

Since the height of the liquid also matters in the experiment, a quick test was conducted to find the appropriate liquid height for cell aggregation. The liquid height tested were 60, 70, 80, 90 uL. No significant difference was observed between the four liquid heights: therefore, we used 70 uL for the other experiments.

The experiment to monitor the temporal evolution of cell aggregate was conducted. Rather than doing all the experiments separately, the wells were kept vibrating for 2 hours and the cell solutions were added every 6 minutes. Then, after two hours, the well plate was transferred to microscope for imaging. In this way, in one experiment the results of various time could be obtained. The results are shown in **Figure 6**. After 42 minutes, the cells were roughly

concentrated, and at 108 minutes, the cells were tightly aggregated. Inner voids, which are expected to lag the spheroid generation time, disappears after 96 minutes.

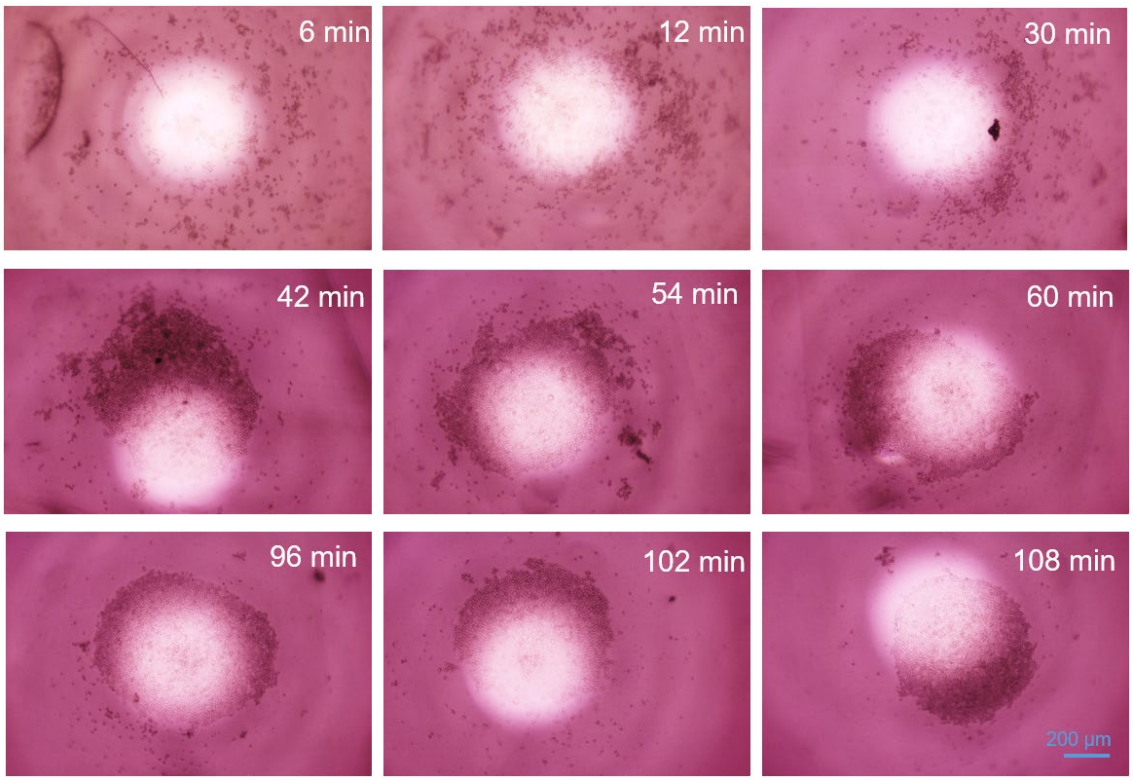

Figure 6. The temporal evolution of cell aggregates

3.2. Comparison to other methods

The efficacy of the vertical vibration method was evaluated by comparing the speed and the aggregate shape to other conventional methods, which are sedimentation method and orbital shaker method.

Figure 7 shows the results of sedimentation method. Near 42 minutes, the cells tend to gather near the middle. Until the experimental time limit of 2 hours, the cell aggregate did not show a round periphery and large voids were observed. However, after 1 day, the cells gathered in circle and the voids disappeared.

Figure 8 shows the results of orbital shaker method. The orbital shaker model we used was Titramax 100, Heidolph Inc., and the angular velocity was set as 300 RPM. Near 30 minutes, the cells tend to gather near the middle. Until the experimental time limit of 2 hours, the cell aggregate showed an oval shape, and voids were present. However, after 1 day, the cells gathered in circle and the voids disappeared.

We wanted to see how long it takes for the cell aggregates to gather tightly as in the vertical vibration setup. As the time flows, the cells slowly turn into a spherical shape for both methods, which took 4~5 hours. The voids in cells

aggregates disappeared after about 4~5 hours in the sedimentation experiments. For the shape of the boundary (**Figure 10**), sedimentation method had a vague boundary and the orbital shaker had uneven boundary. The reason is that for the sedimentation method, since the bottom is U-shaped, the tangential component of gravity is very weak near the middle of the bottom (where the aggregate is located). Hence, the cells are distributed sparsely near the boundary. For orbital shaker, since the cells are subjected to periodic centrifugal force, some parts of boundary are pushed (while the other parts are not). In contrary, the vertical vibration, even only after 1.5 hours of shaking, the cells were closely packed at the boundary.

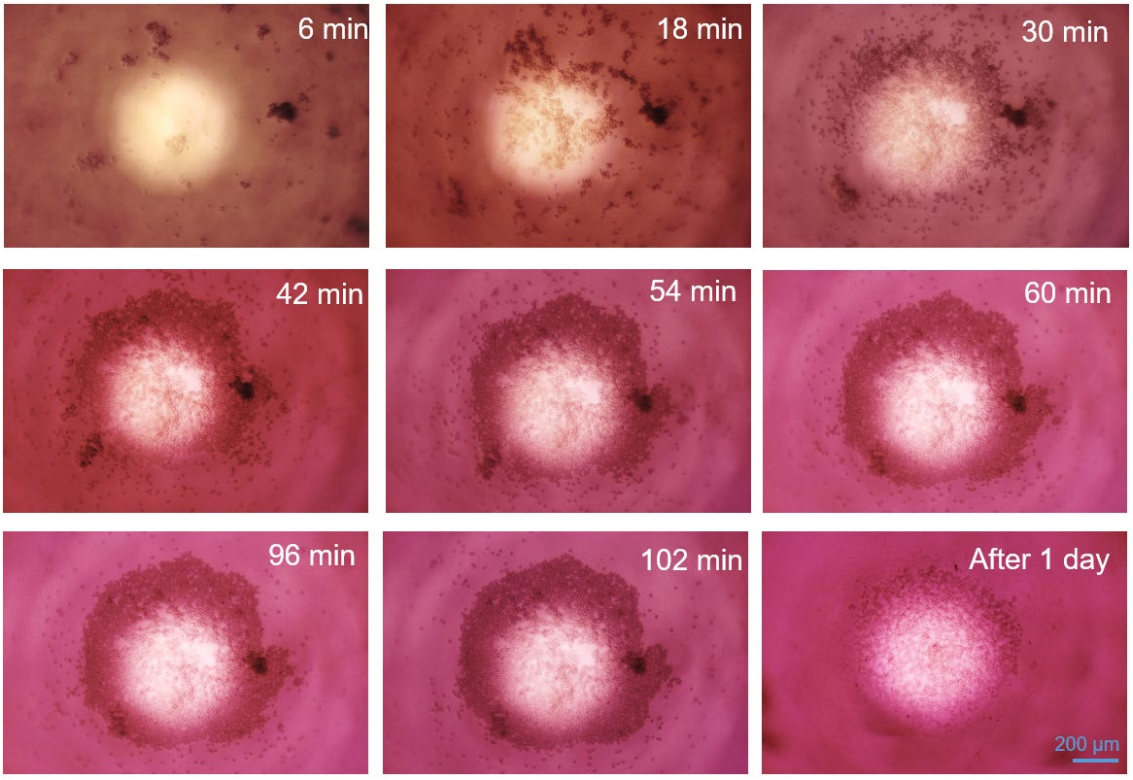

Figure 7. The temporal evolution of cells in sedimentation method

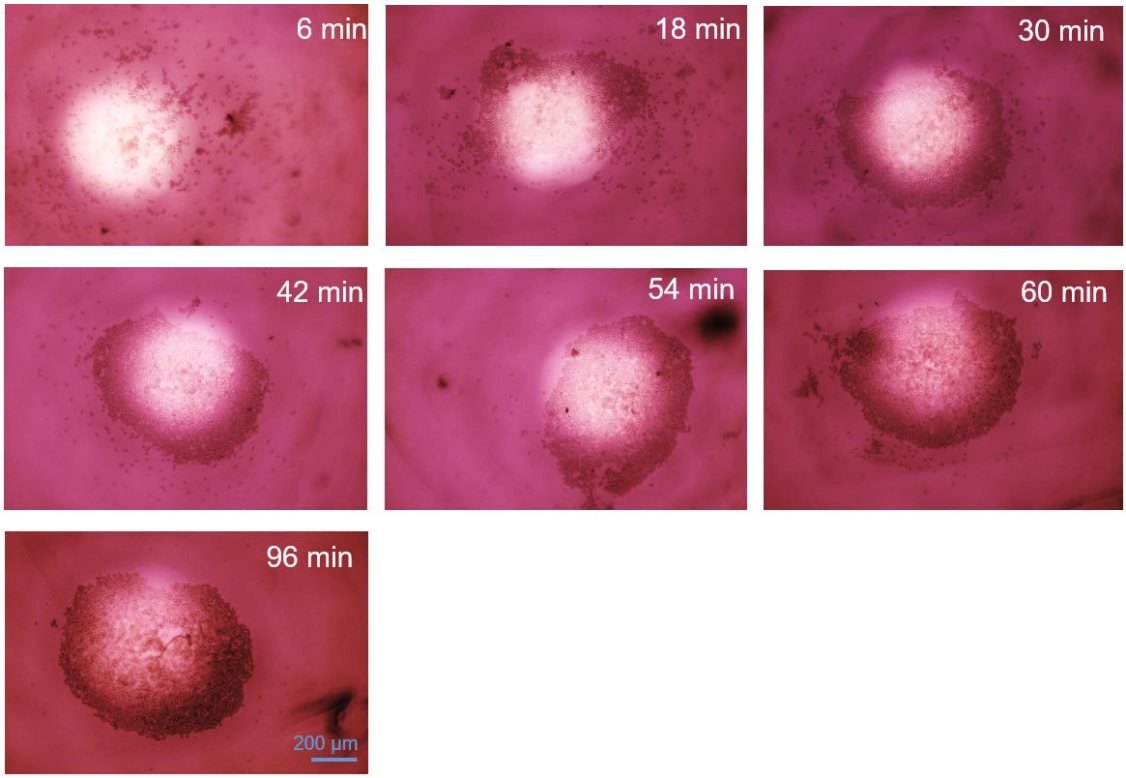

Figure 8. The temporal evolution of cells in orbital shaker method

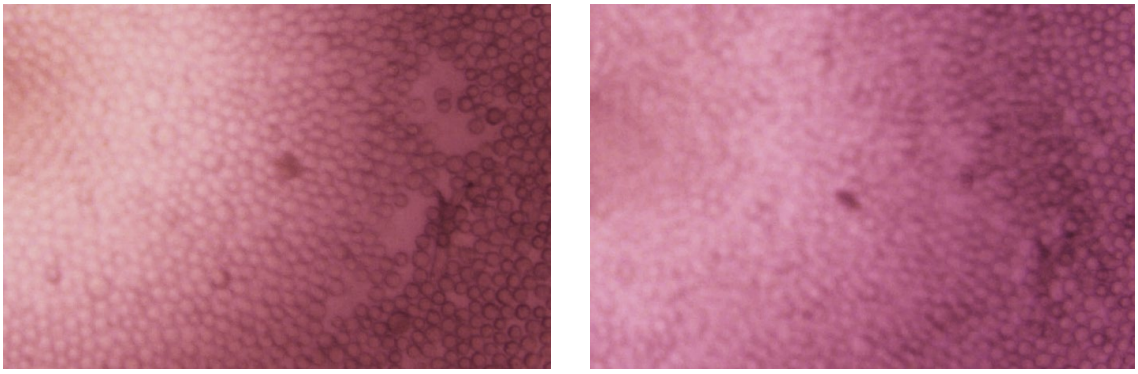

Figure 9. Void formation in sedimentation methods. (a) after 1 hour; voids are very distinct (b) after 4 hours; only small voids present

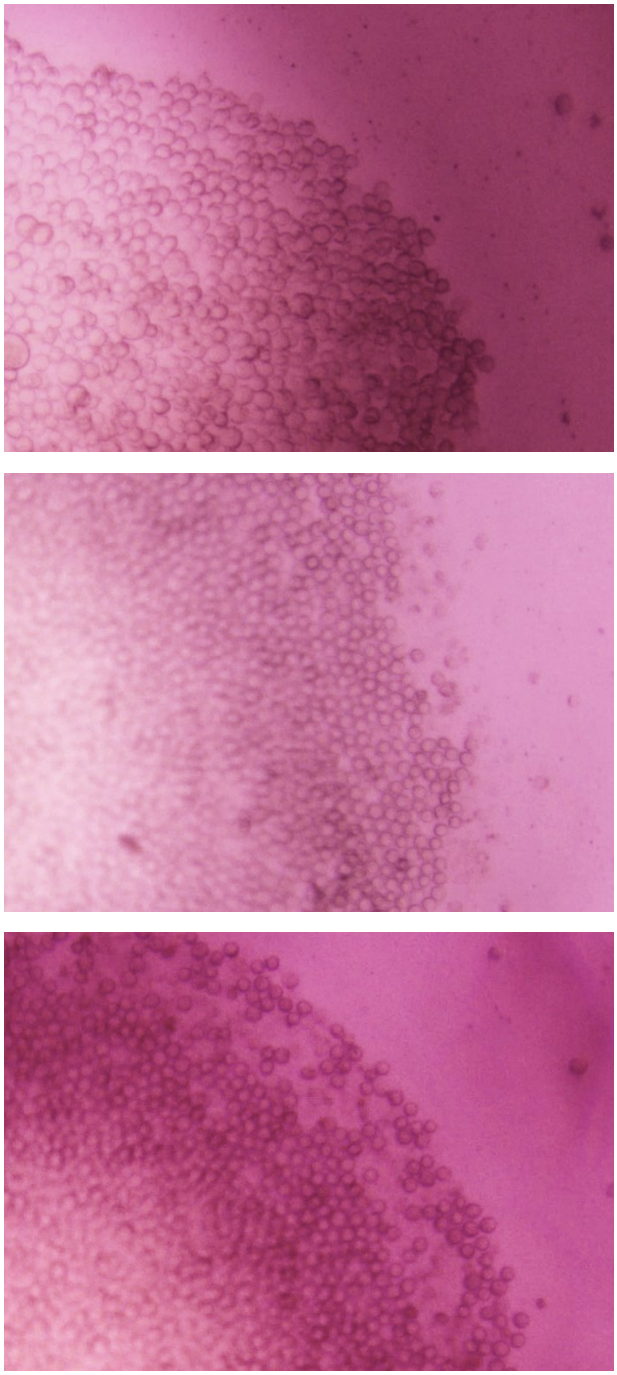

Figure 10. Boundary shapes of aggregates in three methods (a) vertical wave (b) sedimentation (c) orbital shaker

3.3. Cell viability confirmation

During the cell aggregation process, cells are subjected to vibration for more than one hour. For the resulting spheroid to be in use for the real drug development process, the cell viability should not be affected by the cell vibration process.

After 2 hours of vibration, the live cells were dyed in green (Calcein AM), and the dead cells were dyed in red (Propidium Iodide). The confocal microscope image was superpositioned through the height. The results are shown in **Figure 11**. The red cells in both results are barely detected, where only a few of them located outside of the aggregates.

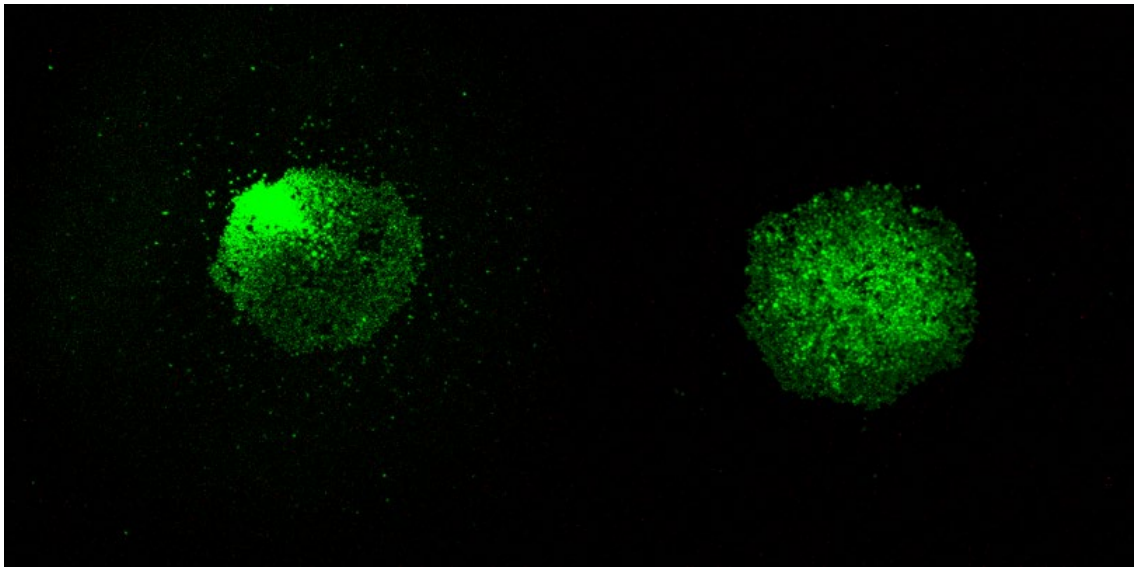

Figure 11. The confocal microscope image of the aggregated cells. Most of the cells are green, indicating that the cells are alive.

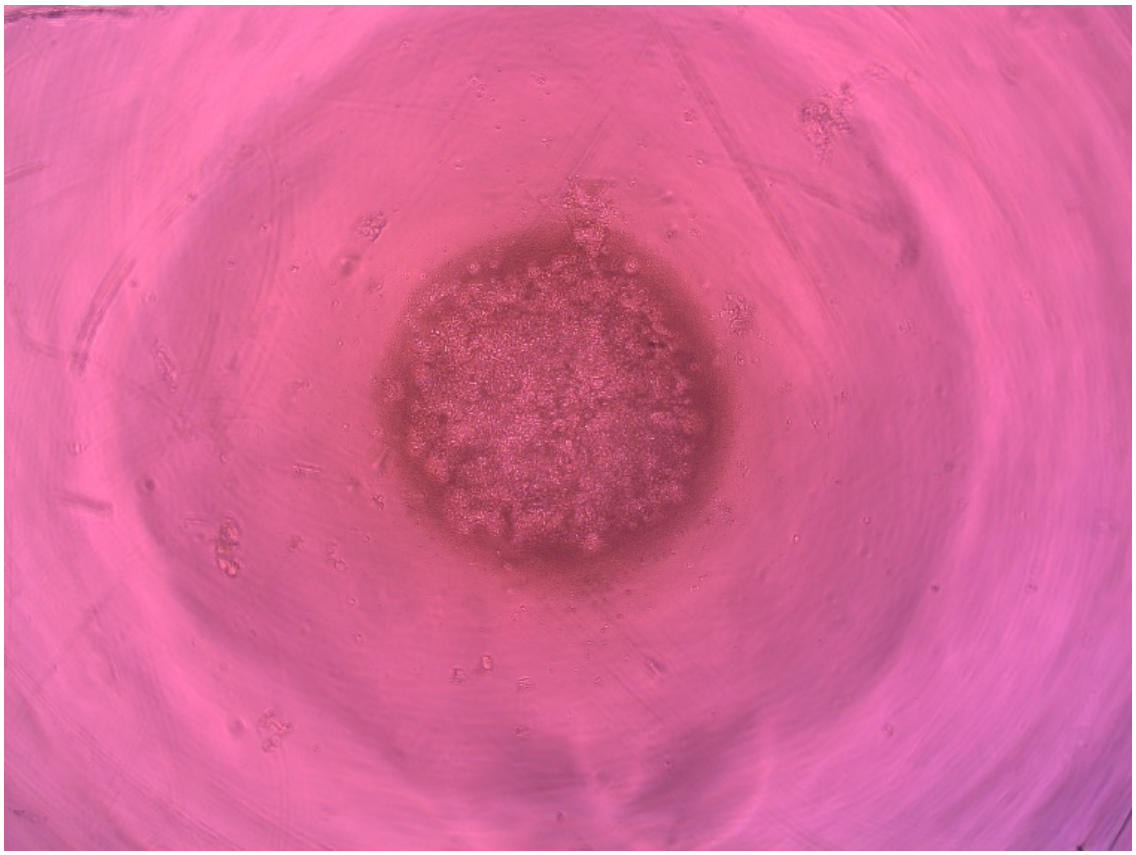

Figure 12. Top−down image by brightfield microscopy.

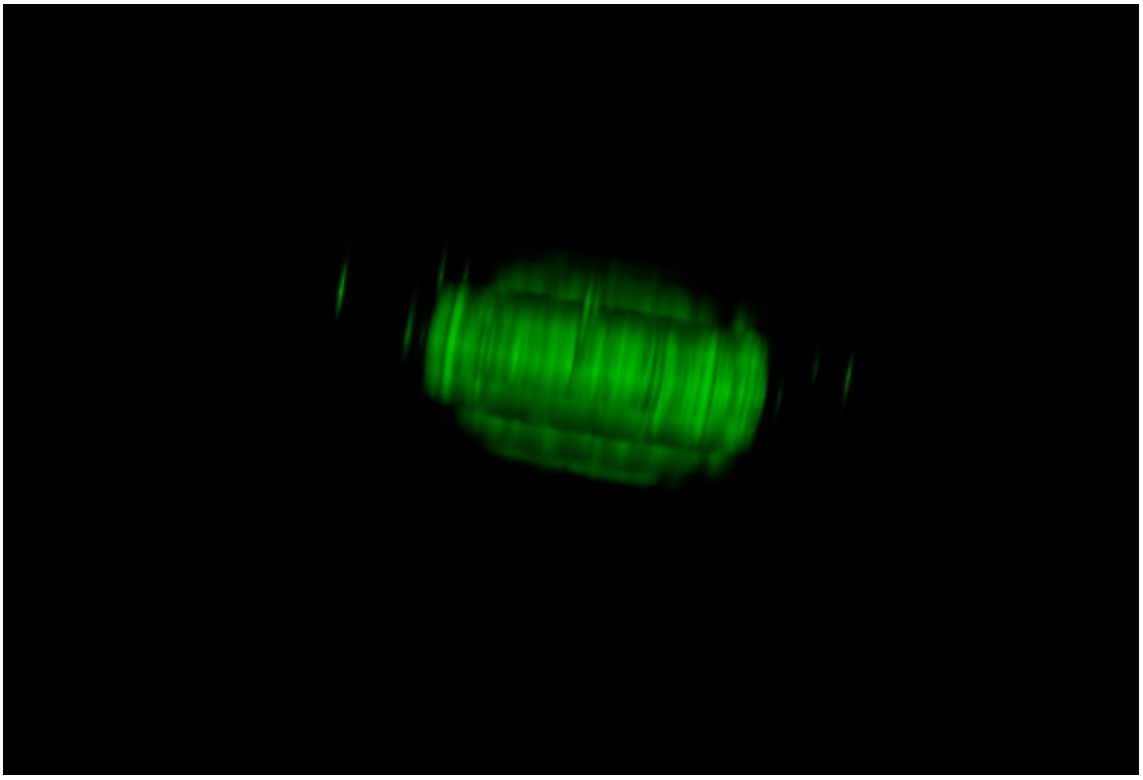

Figure 13. Laminated figure of the confocal images. The aggregate has a shape of hemisphere.

3.4. Mode of failures

Since the flow field is governed by contact line movement and contact angle hysteresis, the result is very dependent upon the contact line status.

For example, if there are some surface contamination on the wall, some parts of the contact line get pinned, and the axis symmetry of the streaming flow breaks.

Also, when bubbles are made during pipetting, the presence of bubbles distracts the meniscus and the cell does not aggregate properly. (Figure 14)

Therefore, to prevent failures, the walls should be cleansed and sufficiently wetted, and the liquid should be homogeneous.

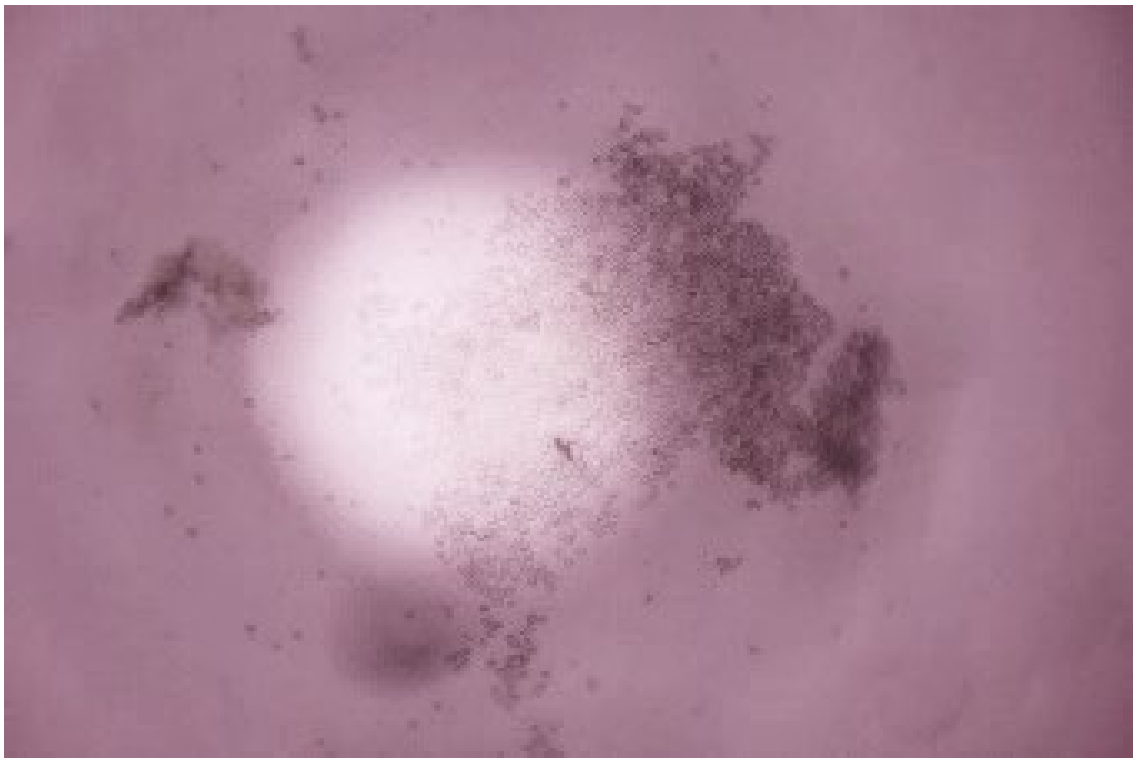

Figure 14. The improper cell aggregation mode in the presence of bubbles.

4. Analysis of the flow and cell aggregation

4.1. Analysis method of the system

The complex nature of fluid flow conceals rich underlying physics, such as a phase shift of π/2 (which should not occur in a forced oscillation with low viscous (damping) term) and intriguing particle aggregation results (the local flow at the bottom can be estimated as a viscous stagnation flow, *i.e.* Hiemenz flow; However, by solving the similarity solution of the Hiemenz flow and inserting it into the equation of motion for particles in the flow, the net force that the particle experiences becomes zero). At the time of writing, the only possible explanation is through computational approaches using a commercial package, COMSOL Multiphysics.

The Navier-Stokes equation was solved using the ALE (arbitrary Lagrangian-Eulerian) method to describe the deforming liquid domain of the system. The simulation was conducted in a 2D, axisymmetric domain to take advantage of the axisymmetric experimental results. The mesh was auto-generated by COMSOL with additional refinements at the contact line, where

abrupt changes occurred due to contact line hysteresis, and at the bottom where cell aggregates formed. Third-order elements were used for velocity components and second-order elements were used for pressure fields. The vibration of the well was converted into a fictitious body force exerted on the fluid in a sinusoidal form. The fluid density was set to 1000 kg/m3, viscosity to 1.5 mPas, and surface tension to 42 mN/m.

4.2. Boundary conditions

For the symmetric axis, the symmetry boundary condition $\frac{\partial u}{\partial n} = 0$ was assigned. For the walls, a very small slip length of 10 um was used (no-slip boundary conditions resulted in very low convergence of the simulated results). For the free surface, the surface tension value was converted into a pressure jump condition. Contact angle hysteresis was assigned as a function of velocity (since contact line motion depends on the interaction between the surface and liquid, this relationship was obtained from experiments: Figure 15).

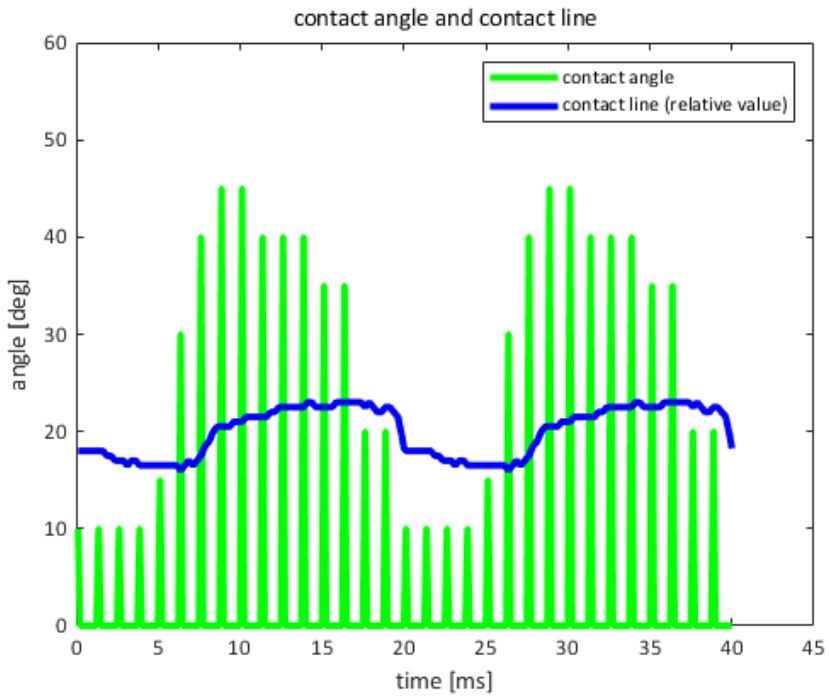

Figure 15. Contact angle hysteresis data and contact line height

4.3. Simulation results

The velocity field was computed, and the time averaged value was computed to compare the results with the experiment. The computational results by COMSOL was in fair agreement with the experiment result: the positions of the vortices were the same and flow direction was same, too. (Figure 16)

The forces on the particle were computed by the equation proposed by Maxey & Riley.

$$m\frac{dv_i}{dt} = mg_i + V\left(\rho_c\frac{Du_i}{Dt} - \rho_c g_i\right) + 3\pi\mu D\left(u_i - v_i + \frac{D}{24}\nabla^2 u_i\right)$$
$$+\frac{1}{2}\rho_c V\frac{d}{dt}\left(u_i - v_i + \frac{D}{24}\nabla^2 u_i\right) + \frac{3}{2}\pi\mu D^2\int_0^t \frac{\frac{d}{d\tau}\left(u_i - v_i + \frac{D^2}{24}\nabla^2 u_i\right)}{\pi\nu_c(t-\tau)^{\frac{1}{2}}}d\tau$$

Comparing the order of magnitudes, only the terms accounting for the Stokes drag and the Faxen force remains.

$$\frac{dv_i}{dt} = 3\pi\mu D\left(u_i - v_i + \frac{D}{24}\nabla^2 u_i\right)$$

The force is dependent to the particle velocity, v_i. However, according to the simulation results, the magnitude of u_i is hundredfold smaller than $\frac{D}{24}\nabla^2 u_i$. Also, the Stokes number is very small and the momentum response timescale of the particle $\left(\tau = \frac{\rho_d D^2}{18\mu}\right)$ is less than 10^{-5} s, which is negligible compared to the period, 0.02 s. Therefore, the fluid velocity and particle velocity are nearly

similar, meaning that the magnitude of $u_i - v_i$ will be much smaller than that of u_i. Then, the equation of motion for the particle can be reduced a simple, segregated equation relating the force and the Laplacian of the flow field.

$$\frac{dv_i}{dt} = \frac{3\pi\mu D^2}{24}\nabla^2 u_i$$

Plotting the Laplacian of the velocity, the force that the particle would experience can be obtained. As the **figure 17** denotes, Laplacian of the velocity components are all negative near the bottom, indicating that the forces head toward the center.

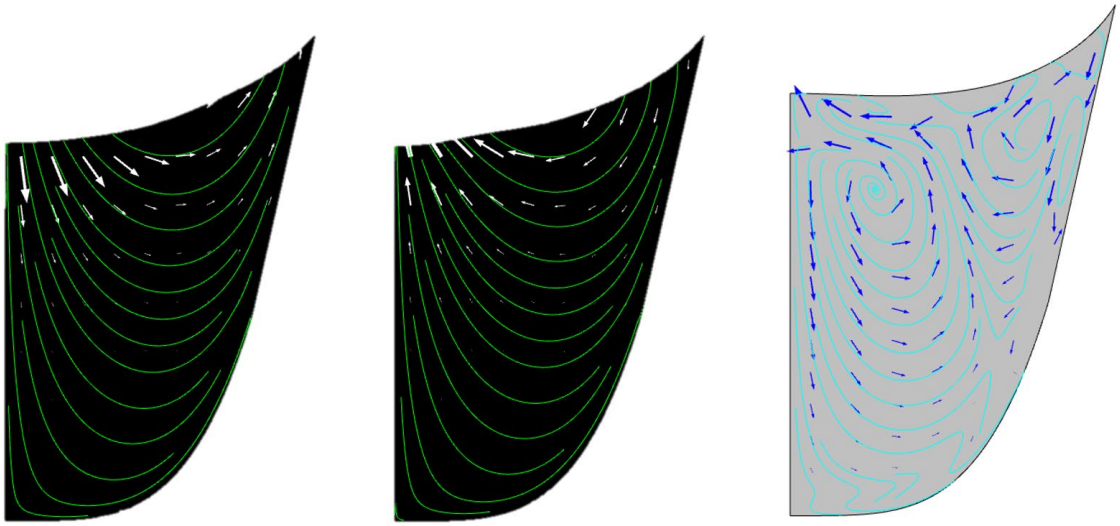

Figure 16. Flow simulation results. (left) The flow field when the flow is at its maximal downward velocity; (middle) the flow field when the flow is at its maximal downward velocity; (right) time-averaged velocity field.

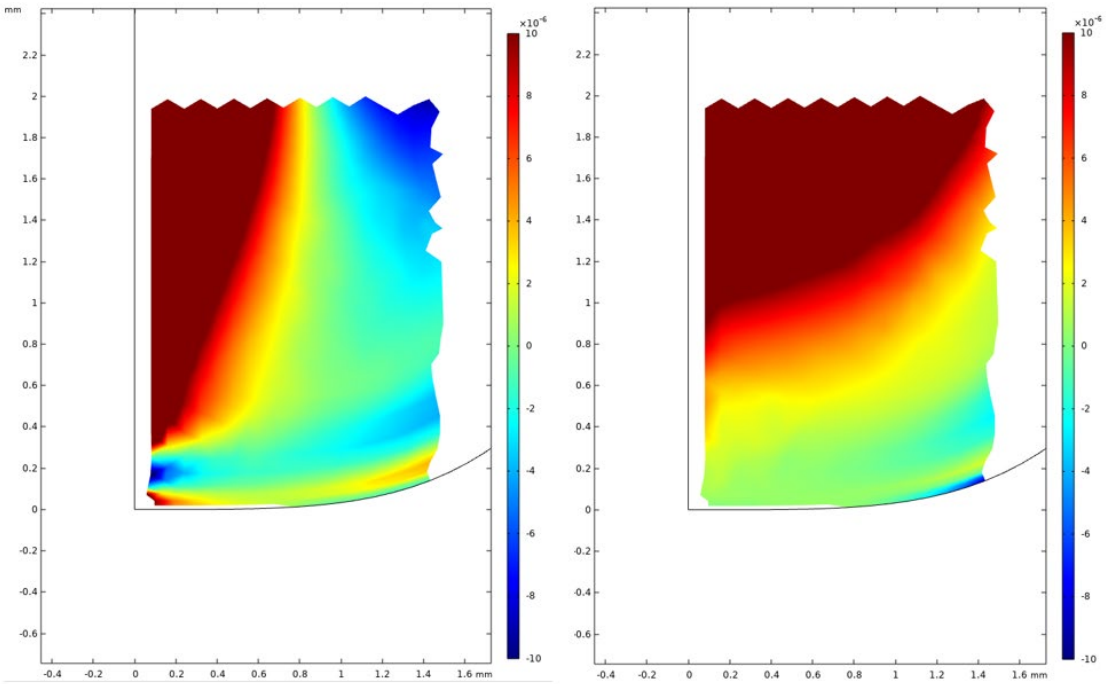

Figure 17. Laplacian value of r−component (left) and z−component (right) of the velocity field.

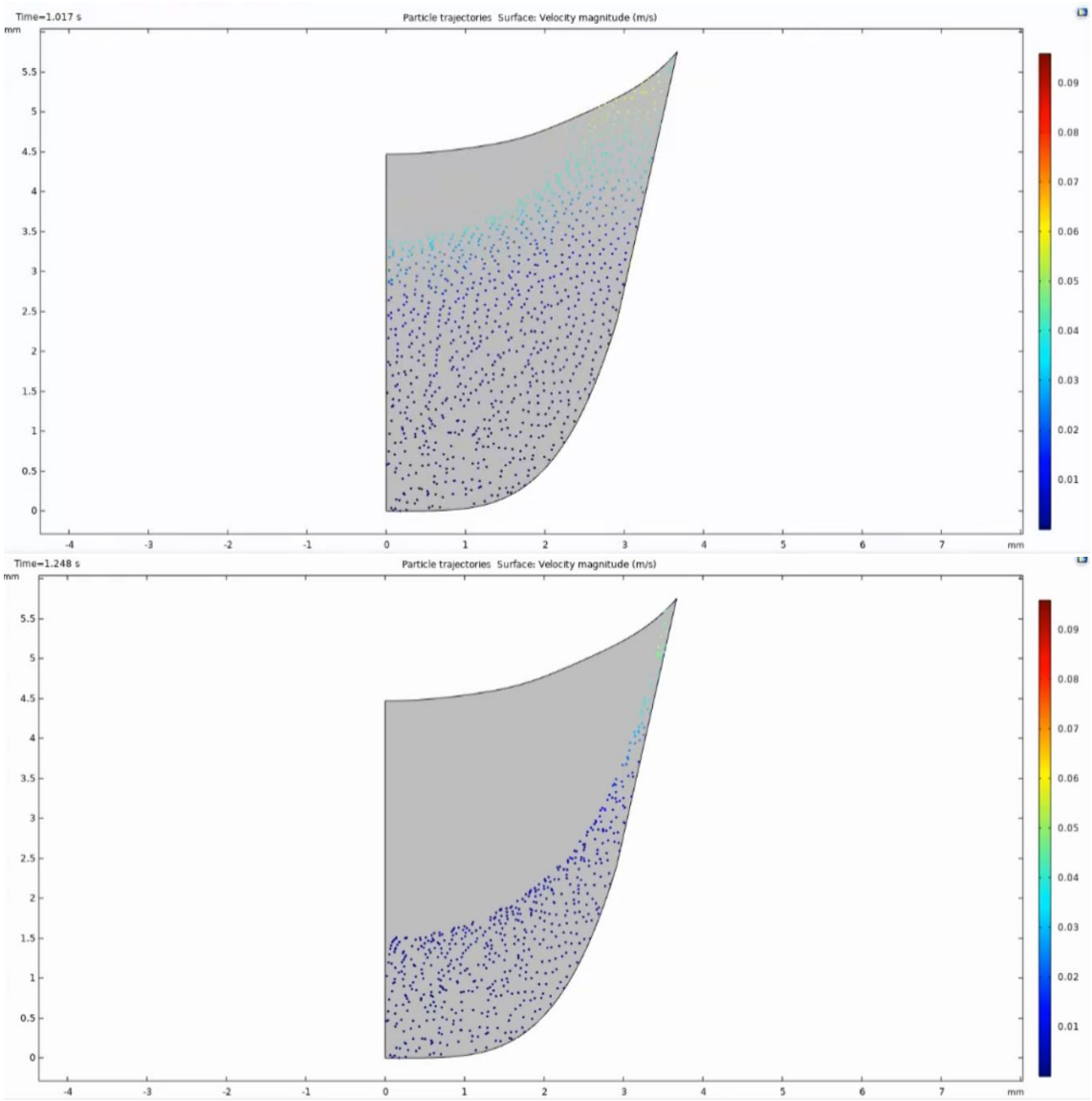

Figure 18. Particle simulation results by particle tracing module in COMSOL Multiphysics (a) 1.017 seconds (b) 1.248 seconds

5. Conclusion

The research proposed a new method using vertical vibrations to aggregate cells rapidly without giving any lethal effects to the cells. The speed and the quality of cell aggregates generated by the method was much faster than the conventional methods. The streaming flow was analyzed using a high-speed camera technique, and the time averaged processing revealed that the streaming flow generates a torus shaped vortex. A simulation with commercial package COMSOL showed results in agreement with the experiment. However, the theoretical explanation was not proposed, which would require some additional studies.

참고 문헌

(1) Kamb, Alexander, Susan Wee, and Christoph Lengauer. "Why is cancer drug discovery so difficult?." *Nature reviews Drug discovery* 6.2 (2007): 115-120.

(2) Riley, Norman. "Steady streaming." *Annual review of fluid mechanics* 33.1 (2001): 43-65.

(3) Périnet, Nicolas, et al. "Streaming patterns in Faraday waves." *Journal of Fluid Mechanics* 819 (2017): 285-310.

(4) Moriarty, Peter, and R. Glynn Holt. "Faraday waves produced by periodic substrates: Mimicking the alligator water dance." *The Journal of the Acoustical Society of America* 129.4 (2011): 2411-2411.

(5) Liu, Dan, Sixun Chen, and May Win Naing. "A review of manufacturing capabilities of cell spheroid generation technologies and future development." *Biotechnology and Bioengineering* 118.2 (2021): 542-554.

(6) Cai, Zheren, and Yanlin Song. "Implementing Contact Angle Hysteresis in Moving Mesh-Based Two-Phase Flow Numerical Simulations." *ACS omega* 6.51 (2021): 35711-35717.

Abstract

Rapid aggregation of cells via vertical vibration

황재우 (Hwang, Jaewoo)

기계공학부 기계공학전공(Mechanical Engineering)

The Graduate School

Seoul National University

In this study, we investigated the phenomenon of rapid cell aggregation using flow field generated by the interaction of vertical vibration and surface tension. We found that a streaming flow arises due to the moderate Reynolds number of the vibration system, and the streaming flow showed perfect axisymmetry under vertical vibration. Conducting experiments with real cancer cells, we found out that this axisymmetric, point-directing streaming flow can rapidly and densely gather the cells in the desired point. In addition, we created spheroids and confirmed that there were no major problems with cell viability as well. Through comparison with other methods, it was also proved that this method gathers the cells faster and more densely. Subsequently, we analyzed how this flow is generated and how it makes the cells gather, through theoretical explanation and CFD simulations.

Keywords : spheroid, streaming flow, Faraday waves, particle aggregation

Student Number : 2021-27838